IABSE-JSCE Joint Conference on Advances in Bridge Engineering-IV, August 26-27, 2020, Dhaka, Bangladesh
Amin, Okui, Bhuiyan, Rahman (eds.)
ISBN: 978-984-34-8313-3
www.iabse-bd.org

Designing loose rock riprap to protect bridge piers

D.C. Froehlich
Consulting Engineer, Cary, North Carolina, USA

ABSTRACT: Considering the several ways in which riprap protection at bridge piers can fail, a practical design requires evaluation of the following three items: 1) The maximum depth of general scour around the pier, including an assessment of the fluctuations of the bed level caused by migrating bedforms (e.g., dunes) past the pier, 2) the size of the stone needed to resist the hydrodynamic forces of water flowing around the pier, and 3) the extent and thickness of the riprap blanket placed around the pier. Here the second and third design elements are the center of interest. First, a rational expression is developed for calculating the representative diameter of stable loose stone placed around bridge piers based mainly on potential flow theory. Stability is determined from the ratio of static moments resisting and promoting overturning of a single rock particle, which defines a safety factor. Second, a mathematical model of the deployment of rock riprap falling aprons at bridge piers is developed based on a conceptual kinematic representation of apron formation.

1 INTRODUCTION

The most widely used method for protecting bridge piers against scour consists of placing loose rocks on the surrounding streambed. The process works well, with little loss or subsidence of the stones if the riprap is sized and installed correctly. However, riprap placed around bridge piers to guard against scour does fail. Experimental studies have identified the following ways in which that happens:

1. Shear failure caused by stones not being able to resist the hydrodynamic forces imparted by the stream flow.
2. Winnowing failure caused by erosion of underlying soils through the porous protective layer from the effects of flow turbulence and seepage.
3. Edge failure caused by erosion at the periphery of the riprap apron, which does not extend far enough horizontally to prevent scour, and which is not capable of deploying and armoring the slopes of the resulting scour-hole.
4. Bed form undermining caused by dunes migrating past the protective layer and eroding beneath the edge of the apron.

Considering the several ways in which riprap protection at bridge piers can fail, a practical design requires evaluation of the following three items:

1. The maximum depth of scouring around the pier, including an assessment of the fluctuations of the bed level caused by migrating bed forms (e.g., dunes) past the pier.
2. The size of the stone needed to resist the hydrodynamic forces of water flowing around the pier.
3. The extent and thickness of the riprap blanket placed around the pier.

Here the second and third design elements are the center of interest. First, a rational expression is developed for calculating the representative diameter of stable loose stone placed around bridge piers based mainly on potential flow theory. Stability is determined from the ratio of static moments resisting and promoting overturning of a single rock particle, which defines a safety factor. Flow velocities and the shear stresses they produce are found from a combination of empirical relations and theoretical solutions of the two-dimensional flow field around a cylindrical column.

Second, a mathematical model of the deployment of rock riprap falling aprons at bridge piers is developed based on a conceptual kinematic representation of apron formation. The model, which is founded on results of scale-model experiments of falling apron behavior and on practical experience that has influenced current design theory, accounts for the regularly repeated processes of slope erosion followed by rock settlement that takes place along a receding convex, conical underwater slope. Apron parameters that are quantified include the needed thickness of a horizontal riprap layer, the amount of stone lost during deployment, and the lateral extent of erosion before complete slope coverage is established. The model is straightforward and can be applied without difficulty to design rock riprap falling aprons used to counteract the threat of bridge pier and abutment undermining by scour.

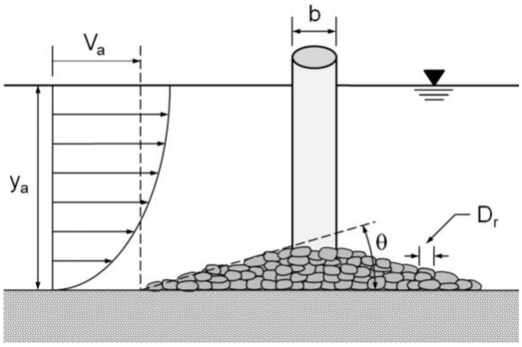

Figure 1. Schematic of the problem of sizing rock riprap to protect a bridge pier.

2 SIZING STABLE ROCK RIPRAP

The general problem of sizing rock riprap to protect a bridge pier is illustrated in Figure 1. The ratio of static moments resisting and promoting overturning of a single rock particle on the side of a riprap mound defines the stability safety factor f_s. For small longitudinal channel and water-surface slopes, Froehlich (2013b) calculates f_s as follows:

$$f_s = \frac{1+\dfrac{\cos\Gamma\tan\theta}{S_r\tan\varphi_r}}{\eta_0\left(\dfrac{1+\sin\Gamma}{2\cos\theta}\right)+\dfrac{\cos\Gamma\tan\theta}{\tan\varphi_r}+\dfrac{1}{S_r}}, \quad (1)$$

where

$$\Gamma = \arctan\left(\frac{1}{2}\frac{\tau_*}{\tau_{co*}}\frac{\tan\varphi_r}{\sin\theta}\right), \ \eta_o = \left(1-\frac{1}{S_r}\right)\frac{\tau_*}{\tau_{co*}}, \ \tau_* = \tau/\left[\left(S_r-1\right)\rho g D_r\right], \quad (2)$$

τ = the shear stress acting on the rock riprap, $S_r = \rho_r/\rho$ = the rock specific gravity, ρ_r = the rock mass density, ρ = the mass density of the ambient fluid (which is considered to be water), g = gravitational acceleration, D_r = the representative rock riprap particle (usually $D_r = D_{50}$ = median intermediate diameter of rocks in a riprap mixture), θ = the side slope angle of the riprap cover, φ_r = the rock riprap mass angle of repose, and τ_{co*} = the dimensionless critical shear stress for a horizontal bed or Shields' parameter (Vanoni 1977), which is approximately 0.06 for turbulent flows (Anderson 1961). The parameter Γ = the angle of rock movement along the slope with respect to horizontal, and the parameter η_o = the particle stability number for flat surfaces and small water-surface slopes, which represents the ratio of shear stress to critical shear stress on a horizontal bed multiplied by the relative difference in the mass density of the riprap and the ambient fluid.

Derivation of Eq. (1) departs from the conventional approach, which is described by Stevens et al. (1976) and Julien (1998), because the buoyant force is not subtracted from the gravitational force to obtain the submerged weight of a particle, which is considered to be a destabilizing force. Instead, the buoyant force is treated separately, and it is split into distinct components that resist and promote overturning, like the conventional treatment of submerged particle weight. A consistent stability factor, which has an upper limit of

S_r, results when gravitational and buoyant forces are considered in this way. As a result, the upper bound of f_s increases in a logically consistent manner as ρ decreases in comparison to ρ_r.

A relation for τ needed to calculate the size rock that will resist overturning moments is provided by Manning's formula (Chow 1959), which is uncomplicated and accepted widely. Combining it with Maynord's (1991) expression for Manning's roughness coefficient n for rock riprap as a function of D_r gives τ as

$$\tau = \rho k_n^2 \left(\frac{D_r}{y}\right)^{1/3} V^2. \qquad (3)$$

from which η_o is found as

$$\eta_o = \frac{1}{S_r}\frac{k_n^2}{\tau_{co*}}\left(\frac{y}{D_r}\right)^{2/3} Fr^2. \qquad (4)$$

where y = water depth, V = depth-averaged velocity, and $Fr = V/\sqrt{gy}$ = Froude number of the flow. The shape and angularity of rock is also a factor that affects particle stability and flow resistance. The effect of rock angularity is accounted for by specified values of the mass angle of repose, φ_r, which is higher for angular rock than rounded rock. From measurements of stockpiled stone, Froehlich (2011) finds that

$$\varphi_r = \begin{cases} 31.8^{\circ}; \text{ for round stone} \\ 34.6^{\circ}; \text{ for subround and subangular stone} \\ 38.4^{\circ}; \text{ for angular stone} \end{cases} \qquad (5)$$

A comparison of measured rock sizes from several small-scale laboratory studies to diameters calculated by Eqs. (1) through (4) shows that a safety factor f_s = 1.25 provides an acceptable margin of error needed for design.

2.1 *Potential Flow around Bridge Piers*

Calculation of η_o by Eq. (4) requires an appropriate velocity in the vicinity of a pier. Here V is estimated using theoretical expressions for two-dimensional, incompressible, inviscid, irrotational flow (that is, potential flow) about solid bodies. A circular cylinder in an unbounded uniform flow is used as an elementary bridge pier against which solutions for piers under other conditions and of different shapes will be compared. The potential flow stream function provides the *average* velocity within a distance $r - b/2$ adjacent to a circular cylinder $\bar{V} = \left[\psi(r) - \psi(b/2)\right]/(r - b/2)$. The maximum *average* speed within a distance $r = D_r$ adjacent to a column of a circular cross-section in a uniform flow as shown in Figure 2 occurs along sides and is calculated as

$$\bar{V} = V_a\left[\left(\frac{b}{D_r}+1\right)\Big/\left(\frac{1}{2}\frac{b}{D_r}+1\right)\right] \qquad (6)$$

where V_a = a uniform approach flow velocity. The value $\bar{V}$ is the depth-averaged velocity acting on a stone and is used to calculate the particle stability number η_o. The maximum theoretical speed along the boundary of a circular cylinder is twice the uniform flow velocity.

Combining Eqs. (1), (3), (4), and (6) gives the following analytical expression for the stable value of D_r at the base of the circular pier:

$$\frac{D_r}{y_a} = K_r \times K_b \times Fr_a^3, \qquad (7)$$

where

$$K_r = \left[\frac{\dfrac{k_n^2}{\tau_{co*}}\left(\dfrac{1+\sin\Gamma}{2S_r\cos\theta}\right)}{\dfrac{1}{f_s}\left(1+\dfrac{\cos\Gamma}{S_r}\dfrac{\tan\theta}{\tan\varphi_r}\right)-\cos\Gamma\dfrac{\tan\theta}{\tan\varphi_r}-\dfrac{1}{S_r}}\right]^{3/2} \qquad (8)$$

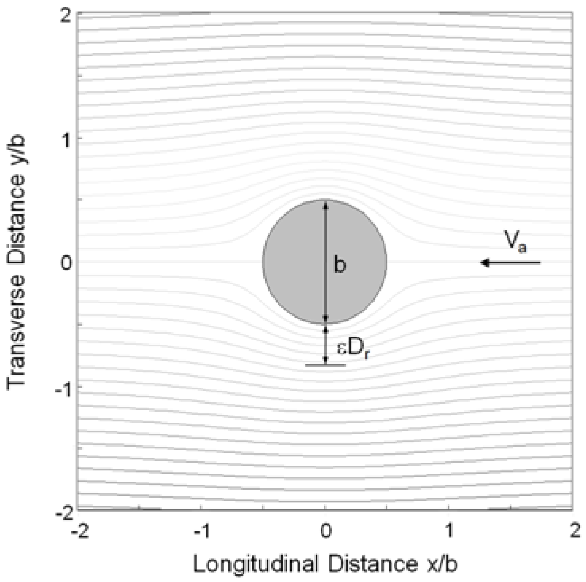

Figure 2. Streamlines around a single unbounded circular column in a uniform flow of velocity Va. Average velocity is calculated over a distance εD_r as shown. The analysis here sets $\varepsilon = 1$.

is a factor that depends on properties of the rock (described by φ_r and τ_{co*}) and its placement (from the specified side-slope angle θ), and the specified degree of safety (defined by the safety factor f_s),

$$K_b = \left[\left(\frac{b}{D_r} + 1 \right) \middle/ \left(\frac{b}{2D_r} + 1 \right) \right]^3 \qquad (9)$$

is a factor that accounts for the relative pier width given by the ratio b/D_r, and $Fr_a = V_a / \sqrt{g y_a}$ = Froude number of the flow approaching the pier. The expression for K_b includes the sought-after rock diameter D_r, thereby necessitating an iterative solution of Eq. (7). For $\theta = 0^o$ (that is, for a horizontal bed), $\Gamma = 90^o$, and the factor K_r given by Eq. (8) reduces to

$$K_r = \left[\left(\frac{k_n^2}{\tau_{co*}} \right) \middle/ \left(\frac{S_r}{f_s} - 1 \right) \right]^{3/2} \qquad (10)$$

3 FALLING APRON DESIGN

A common technique used to guard against erosion at bridge piers is to place a supply of stone around them that will settle or launch down a slope to form a protective facing automatically when the stockpile is undermined. This method was introduced in India during the second half of the 19th century when the first railway bridges were being built across the Ganges River and its tributaries (Bell 1890) and is called a falling or launching apron. A guide on how to apply the falling apron technique, which is used often to this day, was established based on many practical applications, as described by Spring (1903). However, the design approach relies on a vague notion of how bank slope coverage develops as a rock apron deploys, and they all lack quantitative detail.

A mathematical model is developed here that provides a sensible, well-reasoned representation of the physical processes that take place as a horizontal rock apron launches in stages and then progresses down an eroding curved underwater slope in the shape of a conical frustum. The kinematic model will be developed first for falling aprons placed along the tops of straight embankments deploying onto planar underwater slopes following Froehlich (2009). The model will then be extended to account for the effect of curved slopes, which will provide a means of designing falling aprons around bridge piers.

3.1 *Planar-Slope Model Development*

Falling aprons evaluated here are horizontal blankets of loose rock riprap with a constant thickness T_a that launch in stages as the outer edge of the rock stockpile is undermined by an eroding riverbank (see Figure 3). Each launch stage results in deployment of a single layer of stone from the outer face of the apron, which has length $b = T_a / \sin \alpha$, and a thickness D = average rock particle diameter of the riprap mixture, where α = mass angle of repose of the rock forming the apron. Each launch volume per unit length of the apron is then $V_s = b \times D$.

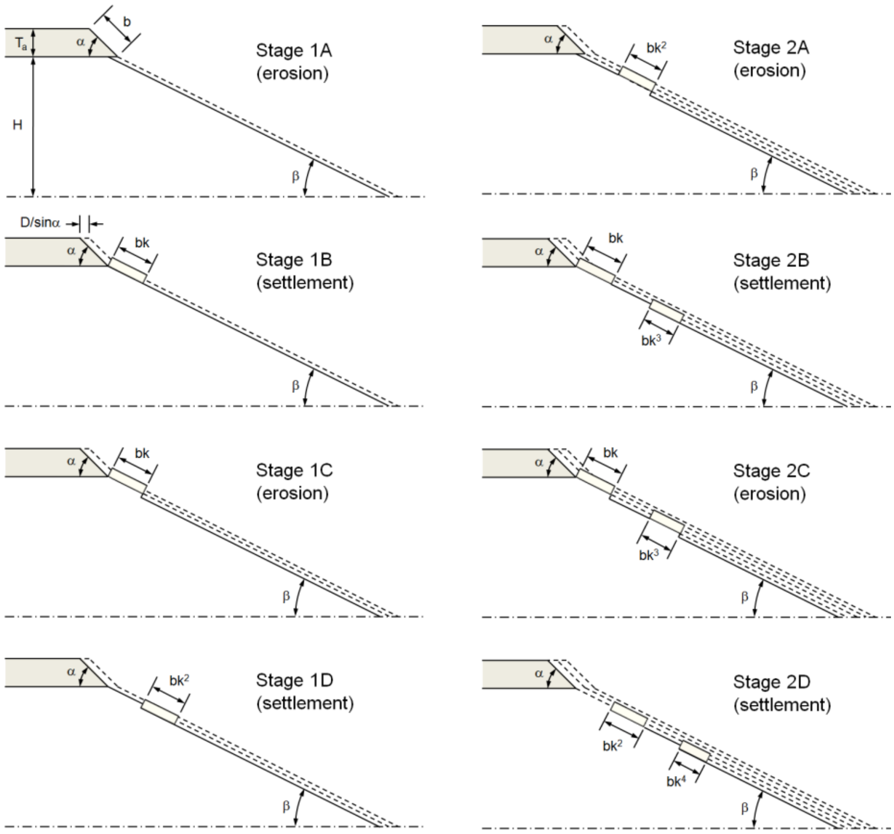

Figure 3. Stages 1 and 2 of apron launching showing the four steps (erosion, settlement, erosion, settlement).

Movement of a launch volume down the bank slope is considered to take place in stages, and each stage is divided into four steps. Step A consists of lateral erosion of the exposed slope immediately below the launch volume by a horizontal distance D. During Step B, the launch volume settles onto the newly eroded slope just below it. In Step C, a second erosion episode takes place on the exposed slope below the launch volume, which is followed by another settlement in Step D.

A launch volume is considered to remain continuous, having an average thickness D as it moves or settles down a slope. If no rock is lost through settlement, the length of a launch volume is constant and equals the length of the apron face b. However, each time a launch volume settles, it is likely that a portion of it becomes buried in the underlying soil and no longer able to protect the slope. Other stones might be swept away by river currents, also becoming ineffective. The fraction of a launch volume that remains after each deployment step (the *retainage* fraction) along a planar slope is denoted by k, where $0 \le k \le 1$. Considering k to stay constant, the length of a launch volume after i stages, each with two settlement steps, is bk^{2i}.

At any stage, before the initial launch volume reaches the bottom of the slope, a channel bank is only partially protected. The cover consists of a series of launch volumes extending down the incline, each of which is separated from the subsequent stage by a gap that has a length equal to that launch volume. Bank soils within the openings between rock volumes are exposed and erode laterally at the same rates. This idea is illustrated by the second stage of apron deployment (Stage 2).

When the initial launch volume reaches the bank toe, no further downward movement takes place if the channel ceases to scour. The following launch volume will then fill the intervening gap at the next settlement step. This process repeats for all the subsequent launch volumes until the final one deploys from the apron face, and the slope is covered entirely by a rock layer of average thickness D.

The total length of slope covered completely by m launch stages is then found as

$$B = b\sum_{i=1}^{m} k^i = \begin{cases} bm; \text{ for } k = 1 \\ b\dfrac{k\left(k^m - 1\right)}{k-1}; \text{ for } 0 < k < 1 \end{cases} \qquad (11)$$

where $B = H \div \sin\beta$, and β = the initial and final bank angle, which is about 2:1 (horizontal:vertical) or 26.6° for sand streambeds. Solving Eq. (11)for the value m gives

$$m = \begin{cases} \chi; \text{ for } k = 1 \\ \dfrac{\ln\left[1 - \left(\dfrac{1-k}{k}\right)\chi\right]}{\ln k}; \text{ for } 0 < k < 1 \end{cases} \quad (12)$$

where $\chi = (H \sin\alpha)/(T_a \sin\beta)$ is a dimensionless fall height factor. As the fraction of rock volume retained at each stage decreases, the number of launch stages needed to obtain complete coverage of a slope increases. Channel banks where conditions result in values of k less than $k_{min} = \chi/(1+\chi)$ would never be able to be covered entirely by stone deployed from the apron because of losses. For this reason, k needs to exceed k_{min} by a suitable margin as a safeguard.

The total volume of rock deployed from an apron is found by summing the separate launch volumes, which are the same for each stage if the apron thickness is constant as has been supposed. The ratio of the total amount of deployed rock to the total amount contained in the final protective bank layer V_b is then found as

$$V_r = \frac{V_d}{V_b} = \frac{\ln\left[1 - \left(\dfrac{1-k}{k}\right)\chi\right]}{\chi \ln k} \quad (13)$$

where $V_b = D \times B = D \times H \div \sin\beta$ = volume of bank cover that is a single rock particle diameter thick. The relation given by Eq. (13) is graphed in Figure 4 for several values of k ranging from 0.75 to 0.975. The graph shows that, for a given k, the deployed stone volume increases for larger values of χ. By expanding the apron thickness T_a, thereby decreasing χ, the amount of stone used to cover a slope completely is reduced, which confirms the U.S. Army Corps of Engineers (USACE) belief that thickness of an apron is the most crucial design factor because it controls the rate at which rock is released in the launching process (USACE 1994, page 3-11). However, a thicker apron increases the vertical load acting on a bank, which increases the potential of bank failure by sliding.

Table 1. Recommended values of rock retainage fraction for planar surfaces based on qualitative descriptions of bank erosion rate and riprap deployment uniformity.

Bank erosion rate	Riprap deployment uniformity	Rock retainage fraction k_p
Slow	Uniform (even)	0.95
Slow	Slightly irregular (uneven)	0.90
Moderate	Slightly irregular	0.85
Rapid	Slightly irregular	0.80
Rapid	Highly irregular	0.75

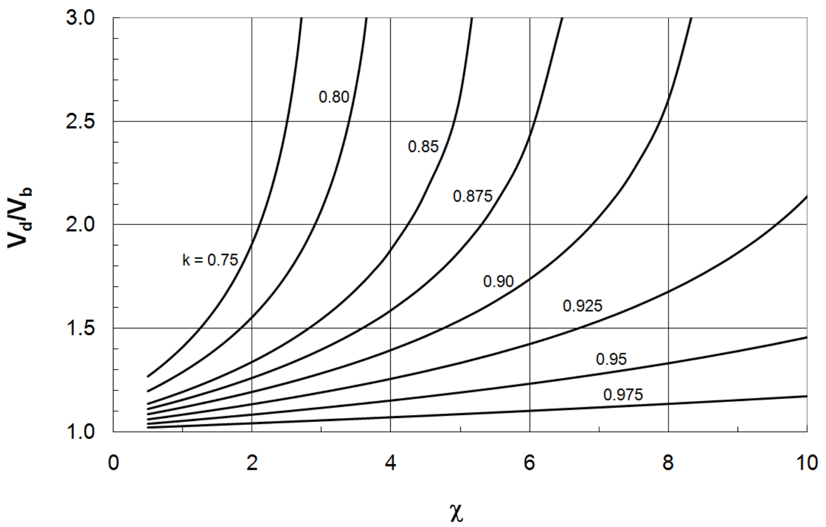

Figure 4. Graph showing relation between the ratio of deployed apron volume V_d to the volume needed to cover the eroded bank completely V_b as a function of the fall height parameter χ and the fraction of retained stone in a launch volume after each deployment step.

From the published results of experimental studies, and from common design practice, *k* ranges from 0.75 to 0.95. Smaller values of k_p apply to conditions that give rise to more significant rock loss, such as uneven launching of stone because of the presence of cohesive soils beneath the apron, rapid erosion of the bank, the tendency for bank slides to occur, or the use of poorly-sorted apron stone. Larger values of k_p apply where bank erosion takes place gradually, bank slides are not likely to happen, and well-sorted stone is used in the apron. Recommended values for k_p based on qualitative descriptions of bank erosion rate and riprap deployment uniformity are summarized in Table 1. When applying Eq. (13) or Figure 4 for planar slopes set $k = k_p$.

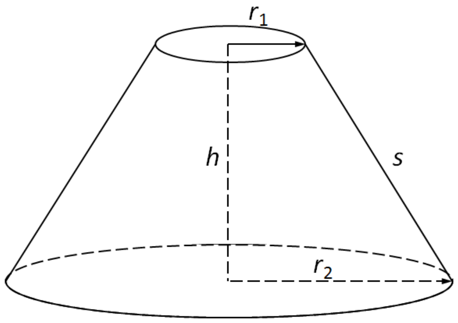

Figure 5. Right-circular conical frustum used to evaluate lateral expansion of rock riprap deployed onto convex slopes.

3.2 *Curved Aprons around Bridge Piers*

Rock riprap falling aprons used to control erosion around bridge piers and abutments will deploy onto convex slopes as the riverbed scours around them. The falling apron design approach presented here for a planar slope surface is modified for application to the curved surfaces surrounding bridge piers and abutments.

Around a bridge pier in the shape of a cylindrical column, the underwater slope that needs to be covered by rock deployed from a falling apron is not a plane but takes the form of a segment of a frustum of a right circular cone as shown in Figure 5. As a result, the farther down the slope a rock deployment moves, the more it must spread out to cover the expanding curved surface, thereby reducing the length of incline that can be protected at each deployment stage. The smaller the radius of curvature of a slope, the higher will be the amount of lateral expansion.

Lateral expansion of stone deployed on a convex bank in effect decreases the planar slope retainage fraction k_p. The conical frustum will be used to evaluate the effect of curved surfaces on rock apron deployment. Side surface area and volume of the frustum is found as

$$A_c = \pi(r_1 + r_2)\sqrt{(r_2 - r_1)^2 + h^2} \text{ and } V_c = \frac{1}{3}\pi h\left(r_1^2 + r_1 r_2 + r_2^2\right), \qquad (14)$$

respectively, where h = height of the frustum, and $r_1, r_2 =$ frustum top and bottom radii. For the initial deployment from the face of the apron, $r_2 = r_1 + h_o \div \tan\beta$, where h_o = the vertical distance covered by the initial launch. Letting $r_1 = R_o$ = the initial radius of curvature at the riprap apron toe, the initial rock volume deployed from the apron face, and the amount deposited on the curved slope, are calculated as

$$V_{do} = 2\pi D\left(R_o - \frac{T_a}{2\tan\alpha}\right)\frac{T_a}{\sin\alpha} \text{ and } V_{bo} = 2\pi D\left(R_o + \frac{h_o}{2\tan\beta}\right)\frac{h_o}{\sin\beta}, \qquad (15)$$

respectively. Equating V_{do} and V_{bo} and solving for h_o yields

$$h_o = \left[\sqrt{1 + \frac{T_a\cos\beta}{R_o\sin\alpha}\left(2 - \frac{T_a}{R_o\tan\alpha}\right)} - 1\right]R_o\tan\beta. \qquad (16)$$

When compared to the initial deployment height on a bank without curvature, the retainage fraction for initial deployment on the curved slope is $k = k_v k_p$, where

$$k_v = \frac{h_o/\sin\beta}{T_a/\sin\alpha} = \frac{h_o}{T_a}\frac{\sin\alpha}{\sin\beta} \qquad (17)$$

is the adjustment factor for convex surfaces.

Because the radius of curvature of the outer edge of the apron is a decreasing quantity as more of the rock is deployed, k_v will vary as well, increasing as the bank erodes, but it will change only by a small amount from the initial to the final deployment for typical conditions. For this reason, k_v given by Eq. (17) with h_o obtained from Eq. (16) is considered to be a constant value for the entire falling apron deployment. When designing falling aprons to protect convex slopes, Eq. (13) or Figure 4 can be used with $k = k_v k_p$ to obtain the ratio of the deployed volume of apron stone to the amount retained on the eroded bank $V_r = V_d/V_b$.

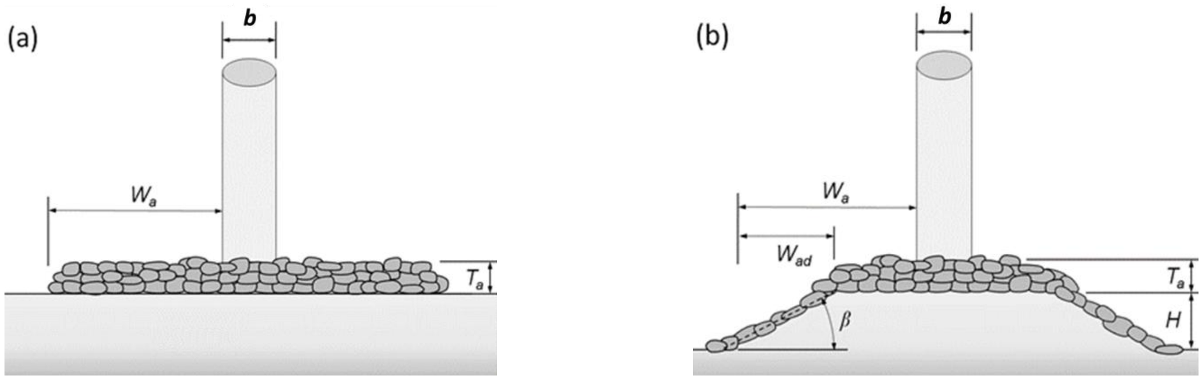

Figure 6. Illustration of a rock riprap falling apron surrounding a bridge pier (a) before and (b) after deployment.

The ability of a falling apron to spread laterally and to completely cover the eroding slopes, as shown in Figure 6, can be determined from Eqs. (16), (17), and (13) given the values of R_o, T_a, D_r, H, α, and β, where $R_o = W_a + b/2$ = the initial apron radius. The fall height H needs to be determined separately from an analysis of scour potential. The representative diameter D_r of rock riprap that will be stable on the covered slopes also must be calculated independently (Froehlich 2009, 2013a).
Considering the surface to be protected by launched riprap to form a conical frustum as shown in Figure 6, the volume of stone deployed from the apron and the amount deposited on the curved surface of the protected bed surrounding the pier, are calculated as

$$V_d = \pi T_a \left(R_o - R_d\right)\left(R_o + R_d - T_a \cot\alpha\right) \text{ and } V_b = \pi DH\left(2R_d + H\cot\beta\right)\csc\beta, \quad (18)$$

respectively, where $R_d = R_o - W_{ad}$. Equating the ratio of V_d and V_b by Eq. (18) to V_r from Eq. (13)and rearranging provides the following quadratic equation for R_d/R_o :

$$\left(\frac{R_d}{R_o}\right)^2 + \left(2V_r \frac{D}{T_a}\frac{H}{R_o}\csc\beta - \frac{T_a}{R_o}\cot\alpha\right)\left(\frac{R_d}{R_o}\right) + \left[V_r \frac{D}{T_a}\left(\frac{H}{R_o}\right)^2 \cot\beta\csc\beta + \frac{T_a}{R_o}\cot\alpha - 1\right] = 0 \quad (19)$$

Solving Eq. (19)for the ratio R_d/R_o gives $W_{ad} = R_o - R_d$ = the deployed width of the apron.

4 SUMMARY AND CONCLUSIONS

A rational expression was developed for calculating the representative diameter of stable loose stone placed around bridge piers based mainly on potential flow theory. Stability was based on the ratio of static moments resisting and promoting overturning of a single rock particle, which defines a safety factor f_s. A comparison of calculated and measured rock sizes suggests that $f_s = 1.25$ provides an appropriate margin of error needed for design.

Next, a mathematical model of the deployment of rock riprap falling aprons at bridge piers was developed based on a conceptual kinematic representation of apron formation. The model presents a sensible and realistic quantitative description of the physical processes that take place as a horizontal rock apron launches in stages (where each deployment of stone has a thickness equal to the average rock particle diameter) and then progresses down an eroding planar slope in regularly repeated processes of slope erosion followed by rock settlement.

The falling apron model was extended to evaluate deployment on curved, convex underwater slopes, such as those around bridge piers, by considering the lateral spreading that is needed to cover the expanding surfaces, which are represented byconical frustums. Adequacy of the falling apron thickness, the amount of stone lost during deployment, and the lateral extent of bank erosion before complete slope coverage is established are factors that can be assessed using the mathematical formulation developed here. The model is uncomplicated and can be used to design rock riprap falling aprons that protect bridge piers from scour.

REFERENCES

Anderson, A.G. 1961. Sedimentation. in V. L. Streeter (ed.), *Handbook of Fluid Dynamics*, McGraw Hill, New York, New York.

Bell, J.R. 1890. The continuous bund and apron method of protecting the flanks of bridges for rivers in the Panjab (India).*Technical Paper No. 2B*, Railway Board, Government Printing Office, Simla, India.

Chow, V.T. 1959.*Open-channel Hydraulics*. McGraw-Hill, New York, New York.

Froehlich, D.C. 2009. Riverbank stabilization using rock riprap falling aprons. *River Research and Applications*, 25(8): 1036–1050.

Froehlich, D.C. 2011. Mass angle of repose of open-graded rock riprap. *Journal of Irrigation and Drainage Engineering*, 137(7): 454-461.

Froehlich, D.C. 2013a. Protecting bridge piers with loose rock riprap. *Journal of Applied Water Engineering and Research*, 1(1): 39-57.

Froehlich, D.C. 2013b. Sizing loose rock riprap to protect stream banks. *River Research and Applications*, 29(2), 219-235.

Julien, P.Y. 1998. *Erosion and Sedimentation*. Cambridge University Press, Cambridge, United Kingdom.

Maynord, S.T. 1991. Flow resistance of riprap. *Journal of Hydraulic Engineering*, 117(6), 687-696.

Spring, F.J.E. 1903. River training and control. *Technical Paper No. 153*, Railway Board, Government Printing Office, Simla, India.

Stevens, M.A., Simons, D.B., and Lewis, G.L. 1976. Safety factors for riprap protection. *Journal of the Hydraulics Division, ASCE*, 102(HY5), 637-655.

U.S. Army Corps of Engineers. 1994. Hydraulic design of flood control channels. *Engineer Manual No. 1110-2-1601*, Washington, D.C.

Vanoni, V.A. (ed.) 1977.Sedimentation engineering. *ASCE Manuals and Reports on Engineering Practice No. 54*. American Society of Civil Engineers, New York, New York.